Indian Journal of Biochemistry & Biophysics
Vol. 63, September 2026, pp. 1075-1085
DOI: 10.56042/ijbb.v63i9.32330

Computational identification of potential tissue plasminogen activator (tPA) inhibitors from *Paris polyphylla* phytoconstituents through molecular docking and molecular dynamics simulations for anti-inflammatory therapy

Ghassan Adel Jassim Alkhalifah[1], Sibghatullah Muhammad Ali Sangi[2], Vijayanandhan Venkatesan[3], Sreeharsha Nagaraja[1], Mahalakshmi Suresha Biradar[4], Shankar Mani[4]*, Mohammed Monirul Islam[1], Afzal Haq Asif[1] & Veeriah Chowdary Jasthi[5]*

[1]Department of Pharmaceutical Sciences, College of Clinical Pharmacy; & [5]Department of Oral and Maxillofacial Surgery and Diagnostic Sciences, College of Dentistry, King Faisal University, Al-Ahsa 31982, Saudi Arabia

[2]Basic Medical Sciences Department, College of Medicine, Dar Al Uloom University, Riyadh-13314, Saudi Arabia

[3]Department of Pharmacognosy, MVM College of Pharmacy, Maruthi Nagar, Yelahanka-560 064, Karnataka, India

[4]Department of Pharmaceutical Chemistry, Sri Adichunchanagiri College of Pharmacy, Adichunchanagiri University, B G Nagar-571 448, Karnataka, India

Received 05 June 2026; *revised 21 July 2026*

Plant-derived bioactive compounds exploration presents a good approach to discovering new anti-inflammatory agents. Phytoconstituents of *Paris polyphylla* were explored as an inhibitor of tissue plasminogen activator (tPA) in the present study using an integrated *in silico* strategy. Molecular docking demonstrated that some of the compounds were highly docked to the tPA active site, with Disogluside docking the best (−10.1 kcal/mol) in comparison to the co-crystal ligand (−10.1 kcal/mol) and the reference drug Nimesulide (−7.2 kcal/mol). Interaction analysis revealed that Disogluside was able to establish stable hydrogen bonds with key catalytic residues such as Thr175, Ser195, Gly216 and Gly219, and established strong hydrophobic interactions. The stability of the Disogluside–tPA complex was confirmed by molecular dynamics simulations (200 ns) with stable RMSD and minimal structural fluctuations. In addition, MM-GBSA computations revealed a favorable binding free energy (ΔGbind = −65.04 ± 4.82 kcal/mol), which was primarily driven by van der Waals and lipophilic interactions. The results indicate that Disogluside can be a potential tPA inhibitor with anti-inflammatory implications and should be investigated by additional experiments.

Keywords: Anti-inflammatory activity, Disogluside, MM-GBSA analysis, Nimesulide, *Paris polyphylla*, tPA Inhibitor

Inflammation is a multifaceted biological process that is linked to a wide variety of disease-related pathologies, such as cardiovascular diseases, cancer, and autoimmune diseases. The regulation of major enzymes used in the inflammatory processes is another important therapeutic approach[1]. Tissue plasminogen activator (tPA) is a serine protease mainly engaged in the process of fibrinolysis, which has been gaining recognition as an inflammatory mediator, remodeler of the extracellular matrix, and cellular signaling[2]. Recent data indicate that, in addition to its classical action in fibrinolysis, tPA acts as a key mediator of inflammatory signaling, activating the plasminogen to plasmin cascade, resulting in extracellular matrix destruction and increased immune cell entry[3]. Besides being a proteolytic enzyme, tPA also engages with cell surface receptors, including low-density lipoprotein receptor-related protein-1 (LRP-1) and annexin II, resulting in intracellular signaling pathways, including NF-κB and MAPK pathways[4]. These signaling events facilitate the release of pro-inflammatory cytokines including TNF-α, IL-6 and IL-1β, thus enhancing the inflammatory response[5]. Unregulated tPA has also been linked to higher levels of vascular permeability and tissue destruction which add to the onset of inflammatory diseases even more[6]. Selective inhibition of tPA is, therefore, a promising therapeutic approach to regulate proteolytic as well as signaling elements of inflammation[7].

Natural products in this sense provide a structurally varied and biologically pertinent source of enzyme inhibitors. *Paris polyphylla* is commonly used in traditional medicine in Asia to treat wounds, inflammation, infections, fever, and snake bites. Its rhizomes are especially sought after as anti-inflammatory, analgesic, hemostatic, and detoxifying

*Correspondence:
E-mail: shankarm@accp.co.in (SM); vjasthi@kfu.edu.sa (VCJ)
Suppl. data available on respective page of NOPR

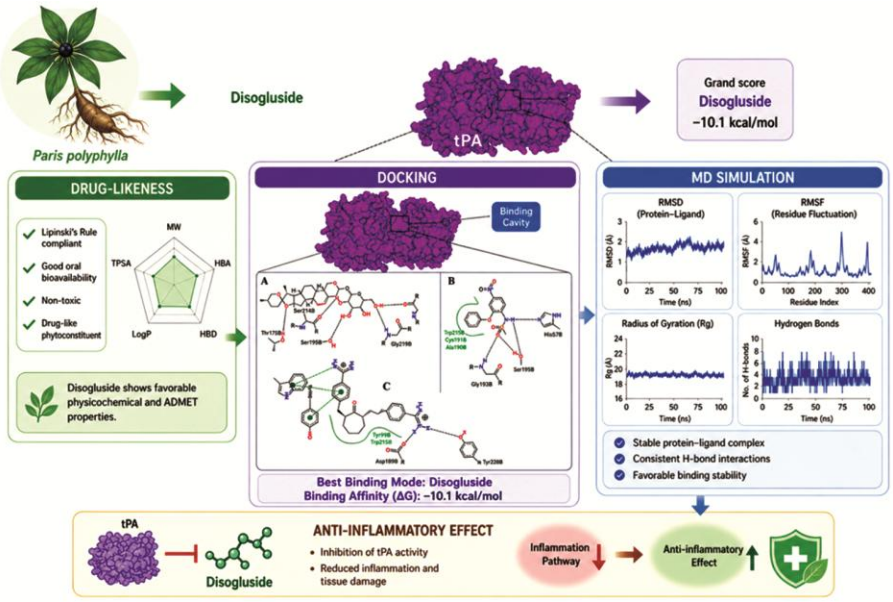

Graphical abstract

agents, and are widely used in cases of tissue damage and haemorrhage[8,9]. Phytochemically, *Paris polyphylla* contains high quantities of steroidal saponins, particularly, polyphyllins (I, II, VI, VII), which are regarded as the main bioactive compounds. It also includes flavonoids, alkaloids, phytosterols and polysaccharides, which contribute to its antioxidant, anticancer and anti-inflammatory effects, which are reported[10].

Computational drug discovery, such as molecular docking, molecular dynamics (MD) simulations, and free energy calculations, has facilitated high-speed screening and mechanistic assessment of bioactive compounds[11]. The methods aid in isolating the possible lead molecules through prediction of binding affinity, stability of interaction and conformational behaviour in the target protein[12].

In this study, we hypothesize that phytoconstituents of *Paris polyphylla* can effectively inhibit tPA through stable binding within its catalytic pocket. To test this hypothesis, an integrated *in silico* workflow involving molecular docking, MD simulation, and MM-GBSA analysis was employed to identify and validate potential inhibitors with anti-inflammatory potential.

Materials and Methods

Ligand retraction and preparation

Phytoconstituents of *Paris polyphylla* were retrieved from the IMPPAT 2.0 database and downloaded in 3D sdf format. All the phyto-constituents were collected from the database available for *Paris polyphylla*. Amino acids, fatty acids, solvents, long-chain hydrocarbons and other incomplete compounds were removed from the collection. Finally, a total of 13 phytoconstituents (mostly saponins) were selected for the docking study. The 3D structures were optimized by adding hydrogen atoms, assigning proper bond orders, and minimizing energy using an MMFF94 force field to obtain stable conformations for docking and simulation studies[13]. Nimesulide is used as a reference drug[14-15].

Protein preparation

The 3D crystal structure of Tissue Plasminogen Activator (tPA) (PDB ID: 1A5H, https://www.rcsb.org/structure/1A5H) was obtained from the Protein Data Bank (Fig. 1a). The experimental resolution of the protein was 2.90Å through X-ray crystallography, and reported no mutation(14). The 3D structure was validated using PDBsum web server (https://www.ebi.ac.uk/thornton-srv/databases/pdbsum/). It provides the Ramachandran plot[16]. The protein structure was prepared by removing water molecules, adding polar hydrogen atoms, assigning bond orders, and assigning the AD4 charge type[17]. AutoDock Tools v1.5.7 was used for protein preparation.

Molecular docking

Molecular docking was performed using AutoDock Vina v1.2.0[18] to evaluate the binding affinity of phytoconstituents toward the active site of tPA. The

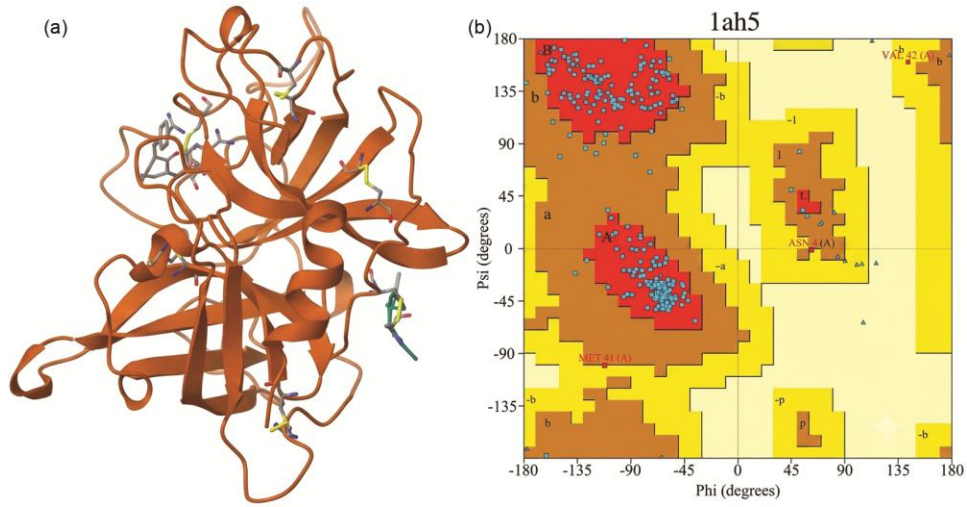

Fig. 1 — (a) 3D structure of 1A5H; and (b) Ramachandran plot depicting the stereochemical quality and backbone dihedral angle distribution (φ and ψ) of the selected protein structure

prepared protein and ligands were converted into the appropriate PDBQT format using OpenBabel v2.4.1[19]. A grid box was defined around the active site based on the co-crystal ligand coordinates to ensure adequate coverage of the binding pocket. The grid box was centered at coordinates (center_x = 17.768, center_y = 52.255, and center_z = 29.564), with dimensions of 20 Å × 20 Å × 20 Å (size_x = 20 Å, size_y = 20 Å, and size_z = 20 Å).

Docking simulations were carried out using 8 exhaustiveness parameters and 10 runs, and binding affinities were expressed as docking scores (kcal/mol). Multiple conformations were generated for each ligand, and the best pose was selected based on the lowest binding energy and favorable interaction profile[20]. The binding interactions of top-ranked ligands were analyzed using BIOVIA Discovery Studio Visualizer 2021 and ProteinPlus server (https://proteins.plus/)[21].

Docking validation

The docking protocol was validated by re-docking the co-crystal ligand into the active site to ensure reliability and accuracy of the docking procedure[22].

Lipinski's rule of five

To ensure the drug-likeness properties, we evaluated Lipinski's rule of five[23] using the Swiss ADME server[24].

MD simulation

The stability of the docked complex was assessed by MD simulations that were implemented on the Schrodinger Desmond simulation package. An explicit solvent model (TIP3P water) was used to embed the protein-ligand complex into an orthorhombic simulation box, and counter ions were added to neutralize the system. The system was reduced and balanced under the NVT and NPT ensembles, and then a 200 ns production simulation was run at 300 K and 1 atm pressure[25].

Trajectory analysis

The stability and dynamics of the complex were measured using post-simulation analyses. To determine the structural stability of both protein and ligand with time, root mean square deviation (RMSD) was calculated. The root-mean-square fluctuation (RMSF) was used to assess the residue-level flexibility of the protein and the ligand's atomic fluctuations. Other parameters such as radius of gyration (rGyr), intramolecular hydrogen bonds (intraHB), molecular surface area (MolSA), solvent accessible surface area (SASA), and polar surface area (PSA) were calculated to determine the compactness of the ligand, its internal stability and the solvent exposure during the course of the simulation[26].

Molecular mechanics generalized born surface area (MM-GBSA) free energy calculation

The MM-GBSA method was used to estimate the binding free energy of the chosen complexes. The value of the calculation was done on representative frames of the MD trajectories based on the Schrodinger Prime module. The overall binding free energy (ΔG bind) and its components, such as Coulombic, Van der Waals, Hydrogen bonding, Lipophilic and covalent binding, were determined to determine the strength and character of ligand protein interactions[27].

Results and Discussion

Protein validation and active site identification

Most of the residues (92.1%) were found in the most favourable regions (A, B and L), suggesting that the protein conformation is of high-quality and energy stable (Fig. 1b). Few residues were found in further allowed and generously allowed regions, whereas very few were found in disallowed regions, indicating minimal steric hindrance or structural strain. The Ramachandran plot offers the accuracy and appropriateness of the protein model to be used in further molecular docking and calculation studies[28].

A native co-crystal docked complex was analyzed, and it exhibited a stable interaction profile with several hydrogen bonds with Thr98, Gly216 and Gly219, and electrostatic interaction with Asp189 (Fig. 2). Also, strong π-π stacking with Trp215 and Tyr99 led to the stabilization of binding in the hydrophobic pocket[14].

Docking results analysis

The binding affinity of the tPA complex to the chosen phytoconstituents of *Paris polyphylla* was determined using a structure-based molecular docking study. The docking scores of the screened compounds were all over -6.2 and -10.1 kcal/mol, showing variable binding affinities in the active site of the target protein (Table 1).

The binding affinity of the evaluated compounds was highest in Disogluside (IMPHY015101), with a docking score of -10.1 kcal/mol, comparable to the co-crystal ligand (-10.1 kcal/mol), indicating that it

Table 1 — Phytoconstituents information and docking score of phytoconstituents against tissue plasminogen activator complex (1A5H) protein

S. No	IMPPAT ID	Phytoconstituents	tPA (1A5H)
1	IMPHY010425	Pariphyllin	-9.6
2	IMPHY009308	Pennogenin	-8.5
3	IMPHY001995	Dioscin	-9.3
4	IMPHY002347	Polyphyllin H	-7.0
5	IMPHY003681	Diosgenin	-8.6
6	IMPHY010214	Polyphyllin-I	-9.7
7	IMPHY000837	Polyphyllin C	-7.1
8	IMPHY003734	Prosapogenin A	-7.6
9	IMPHY007833	Ambrosin	-7.1
10	IMPHY008672	Pariphyllin A	-7.0
11	IMPHY010523	Polyphyllin F	-7.6
12	IMPHY015101	Disogluside	-10.1
13	IMPHY010415	Polyphyllin d	-6.2
14	-	Co-crystal ligand	-10.1
15	-	Nimuslide	-7.2

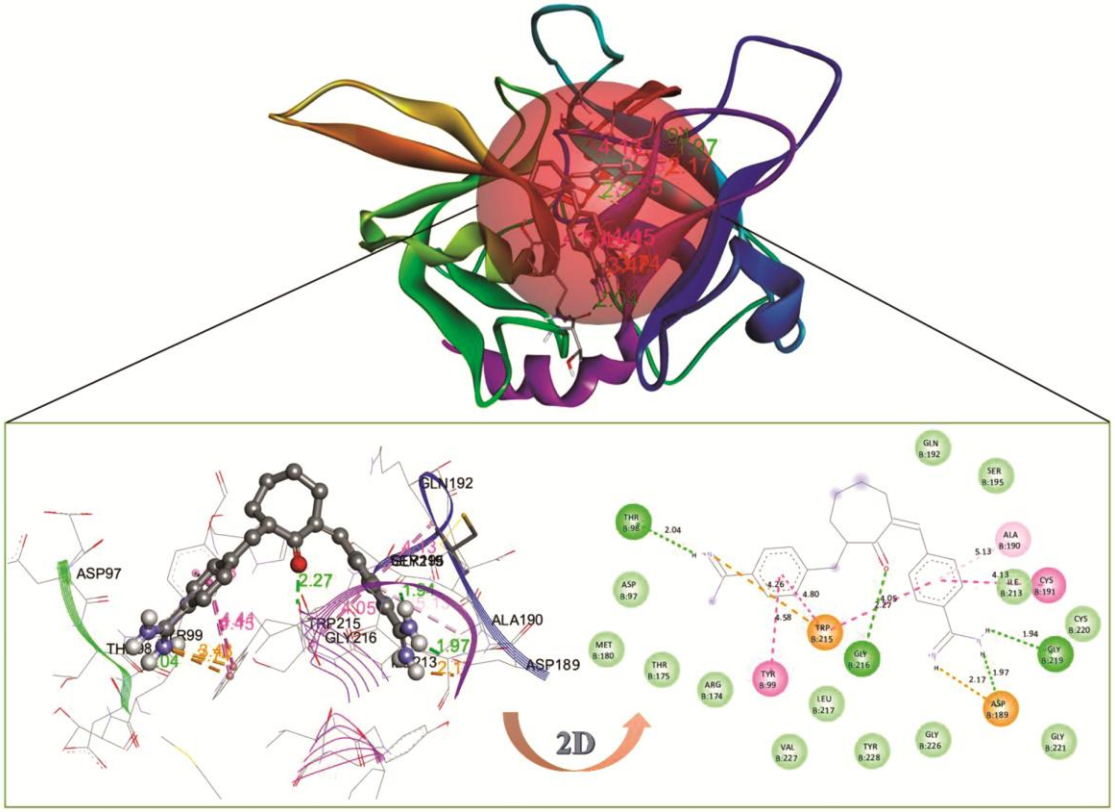

Fig. 2 — 2D representation of native co-crystal ligand interactions within the active binding pocket of the target protein

interacts with the catalytic pocket of the enzyme. Other compounds with significant binding affinities were Polyphyllin-I (-9.7 kcal/mol), Pariphyllin (-9.6 kcal/mol) and Dioscin (-9.3 kcal/mol), which showed stronger interactions compared to the reference anti-inflammatory drug Nimesulide (-7.2 kcal/mol). Also, other compounds, such as Diosgenin (-8.6 kcal/mol) and Pennogenin (-8.5 kcal/mol), had significant binding potential toward the target protein.

Binding analysis

To gain further insight into the ligand binding mechanism, the interaction profile of Disogluside in the active site of tPA was compared with that of the standard drug Nimesulide and the co-crystal ligand (Fig. 3). The protein surface representation demonstrates the well-defined binding pocket, which represents the site of accommodation and stabilization of the ligand molecules.

As depicted in Figure 3a, Disogluside engaged in multiple hydrogen-bond interactions with the active site residues Thr175B, Ser214B, Ser195B, Gly216B and Gly219B. Such hydrogen bonds are crucial in anchoring the ligand within the active pocket. In addition, hydrophobic and π-π stacking interactions were observed with Trp215B and Tyr99B, respectively, which also contribute to the strong affinity observed from docking scores.

In comparison, the reference drug Nimesulide (Fig. 3b) exhibited fewer hydrogen-bond interactions, primarily involving His57B, Ser195B, and Gly193B, along with hydrophobic contacts with Trp215B, Cys191B, and Ala190B. Similarly, the co-crystal ligand (Fig. 3c) demonstrated hydrogen-bond interactions with Asp189B and Tyr228B and hydrophobic interactions with Trp215B and Tyr99B, which are known to contribute to ligand stabilization within the catalytic site. The 2D interaction of all phytoconstituents is given in (Suppl. Figs. S1-S10).

Docking protocol validation

The superimposition of the co-crystallized ligand (green) and the redocked pose (cyan) within the active site of the target protein (magenta cartoon representation) demonstrates a high degree of spatial overlap (Fig. 4). The calculated RMSD value of 2.03

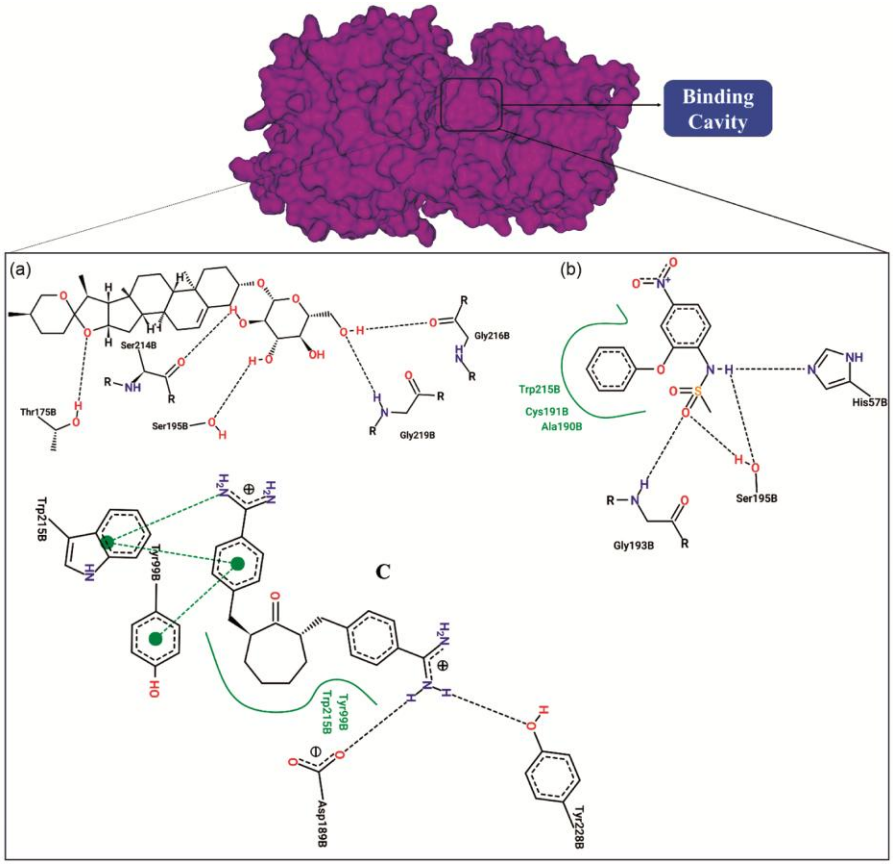

Fig. 3 — 2D molecular interaction profiles of (a) Disogluside; (b) reference drug; and (c) co-crystal ligand within the active sites of tissue plasminogen activator (tPA, PDB ID: 1A5H)

Å suggests good reproducibility of the docking method. The proximity between the key functional groups would suggest accurate modeling of the binding pose of the experimental complex.

Drug likeness properties

The drug-likeness evaluation based on Lipinski's Rule of Five revealed notable variation among the selected phytoconstituents. "Lipinski's Rule of Five states that a compound is more likely to exhibit good oral bioavailability if it has molecular weight ≤500 Da, ≤5 hydrogen bond donors, ≤10 hydrogen bond acceptors, and a logP ≤5, with no more than one violation"[22]. Out of 13 compounds, only four-Pennogenin, Diosgenin, Ambrosin, and Disogluside-satisfied the criteria with zero or one violation, indicating favorable oral bioavailability (Table 2). In contrast, the majority of compounds, particularly Pariphyllin, Dioscin, and various Polyphyllin derivatives, exhibited three violations and were classified as non-compliant.

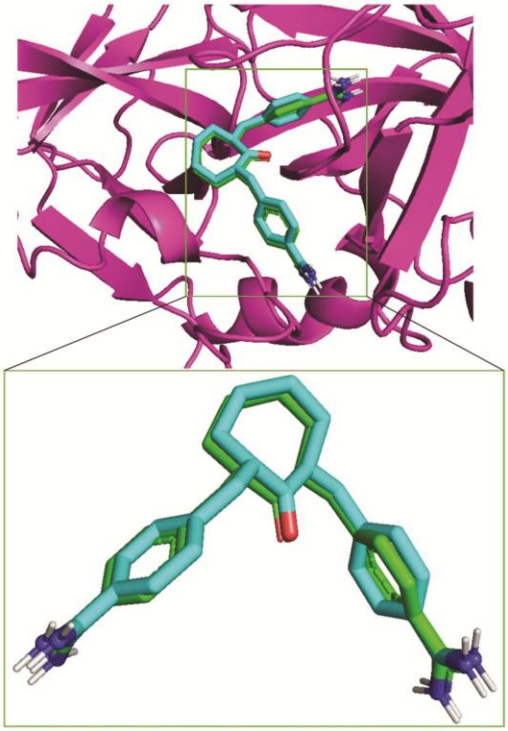

Fig. 4 — Docking validation by redocking

MD simulation

Among the screened phytoconstituents, Disogluside was selected for MD simulation due to its superior docking score (-10.1 kcal/mol) along with acceptable drug-likeness, exhibiting only one violation of Lipinski's rule of five.

RMSD

The stability of the docked complex was evaluated by performing a 200 ns molecular dynamics (MD) simulation of the Disogluside–tPA complex. The 2D representation of the protein backbone RMSD had achieved equilibrium within a few nanoseconds of the simulation, and the RMSD values were mainly in the range of 5.0 to 7.8 Å, suggesting that the protein backbone was relatively stable but still had some conformational flexibility (Fig. 5). The initial 0-90 ns of the simulation showed relatively low ligand RMSD values, in the range of 1.0-1.7 Å, indicating that Disogluside maintained a strong binding within the active site. The conformational rearrangement of the ligand was observed between 90 and 135 ns with a transient increase in RMSD. After this transition, the ligand RMSD settled to around 3.3-3.8 Å for the rest of the simulation, suggesting a new stable binding orientation in the binding pocket. No significant large

Table 2 — Drug-likeness evaluation of selected phytoconstituents based on Lipinski's Rule of Five, indicating the number of violations and overall suitability for oral drug development

S. No	IMPPAT ID	Phytoconstituents	Number of Lipinski's rule of 5 violations	Verdict
1	IMPHY010425	Pariphyllin	3	Failed
2	IMPHY009308	Pennogenin	0	Pass
3	IMPHY001995	Dioscin	3	Failed
4	IMPHY002347	Polyphyllin H	3	Failed
5	IMPHY003681	Diosgenin	1	Pass
6	IMPHY010214	Polyphyllin-I	3	Failed
7	IMPHY000837	Polyphyllin C	3	Failed
8	IMPHY003734	Prosapogenin A	3	Failed
9	IMPHY007833	Ambrosin	0	Pass
10	IMPHY008672	Pariphyllin A	3	Failed
11	IMPHY010523	Polyphyllin F	3	Failed
12	IMPHY015101	Disogluside	1	Pass
13	IMPHY010415	Polyphyllin d	3	Failed

fluctuations after this rearrangement, indicating that the Disogluside–tPA complex was stable during the simulation.

RMSF

The RMSF profile showed that the fluctuations of most atoms in the ligand were low, suggesting limited flexibility inside the binding pocket. The RMSF values calculated with respect to the protein backbone were in the range of 1.4-1.8 Å, suggesting small variations relative to the protein backbone (Fig. 6). On the other hand, RMSF values fitting on the ligand itself were less than 0.6 Å, suggesting that the ligand structure was very stable throughout the simulation. The low atomic fluctuations indicate that Disogluside remains stable in its pose within the active site, consistent with the RMSD results. This analysis further supports that Disogluside can form a stable ligand-protein complex with tPA and could be a potential inhibitor.

To examine the flexibility of individual residues during the simulation, RMSF analysis was carried out on the protein residues of the Disogluside-tPA complex. The RMSF analysis showed that most of the residues showed moderate fluctuations (1.0-3.5 Å), suggesting that the complex system was stable throughout the simulation (Fig. 7). There were some areas of higher fluctuations (peaks around 5-7 Å), which are likely to be flexible loops or terminal residues exposed to the solvent.

Interestingly, residues within secondary structural elements, such as α-helices and β-sheets, exhibited reduced fluctuations, indicating that the protein's secondary structure was maintained during ligand binding. Crucially, no drastic fluctuations were observed in the active-site residues, suggesting the binding of Disogluside did not cause severe distortions in the structure of tPA. These observations further support the dynamic stability of the Disogluside-protein complex, and are consistent with the results of the RMSD and ligand RMSF profiles.

Ligand properties

The ligand RMSD values showed relatively small fluctuations during the simulation, with variations less than ~1.5 Å, suggesting that Disogluside did not deviate significantly from its binding pocket. The rGyr profile remained relatively stable throughout the simulation, indicating that the ligand did not undergo significant changes in its radius of gyration and maintained conformational stability during the trajectory. The analysis of intramolecular hydrogen bonds showed occasional intramolecular hydrogen bond formation in the ligand structure, which may help to stabilise its conformation.

Moreover, the MolSA, SASA and PSA values displayed only slight variations along the trajectory, suggesting stable surface characteristics and solvent accessibility of the ligand during the simulation. The subtle changes in SASA could be attributed to minor conformational changes in the bound ligand (Fig. 8).

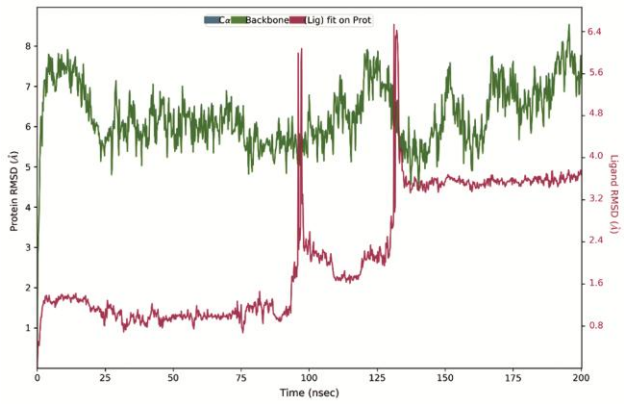

Fig. 5 — RMSD analysis of the Disogluside-tPA complex during 200 ns molecular dynamics simulation

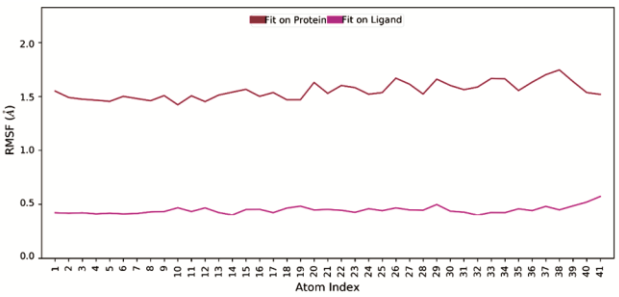

Fig. 6 — RMSF analysis of Disogluside during molecular dynamics simulation with tPA

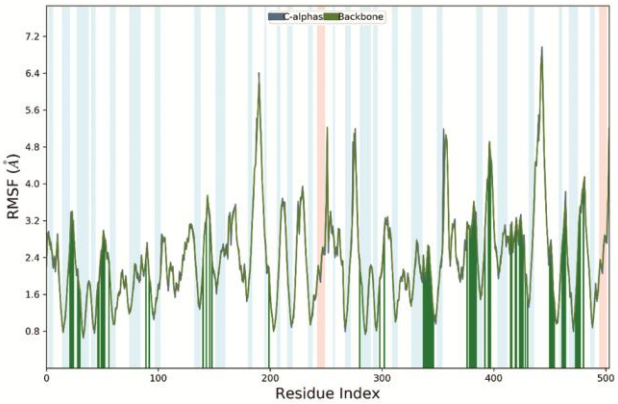

Fig. 7 — RMSF profile of tPA residues during molecular dynamics simulation of the Disogluside-protein complex

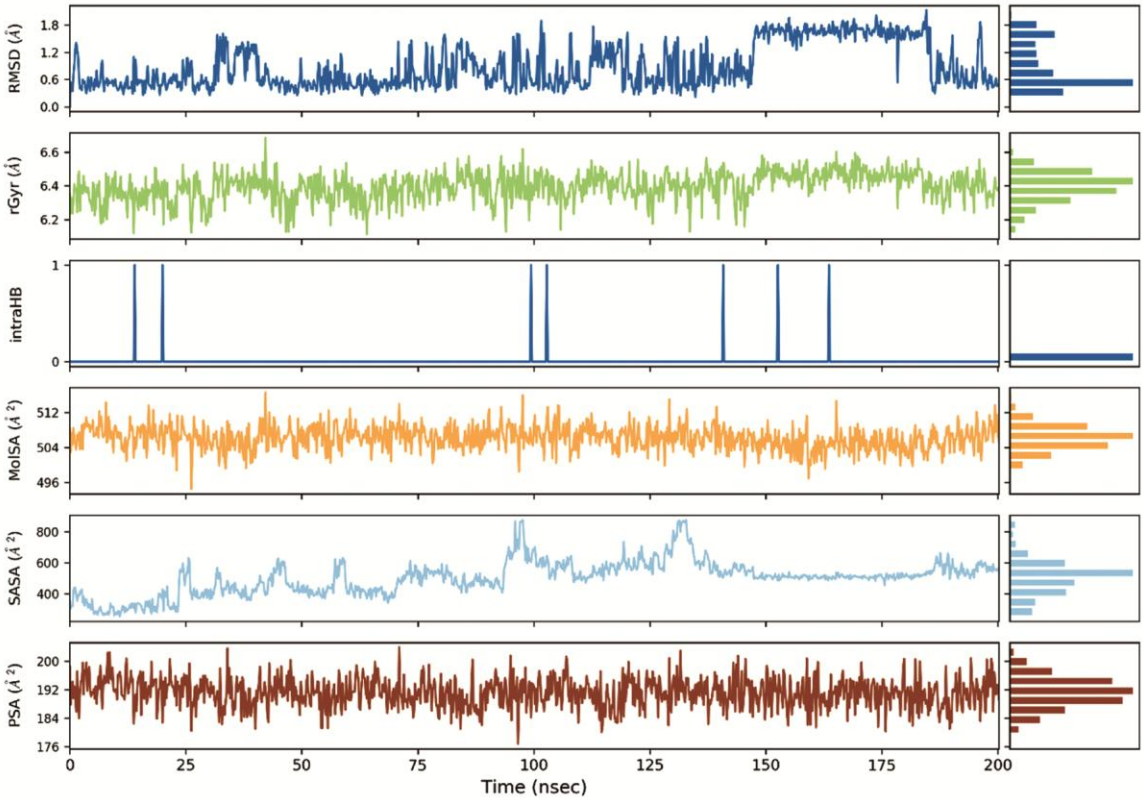

Fig. 8 — Structural and physicochemical stability parameters of the Disogluside-tPA complex during 200 ns molecular dynamics simulation

Protein-ligand complex

A water-bridged hydrogen bond is observed between Disogluside and ARG37A with ~6% occupancy, indicating a relatively weak but stabilizing interaction (Fig. 9a & b). More prominent interactions are seen with GLU60A, where both direct (~16%) and water-mediated (~7–9%) hydrogen bonds are present, suggesting this residue plays a central role in ligand stabilization. Additionally, GLN60A participates in hydrogen bonding (~14%), further contributing to binding affinity. On chain B, ASP132 shows a strong direct hydrogen bond (~18%), representing one of the most significant interactions in the complex. Another water-mediated interaction links the ligand to GLU60B (~9%). Several hydroxyl groups of Disogluside are actively involved in these interactions, emphasizing their importance in anchoring the ligand within the active site.

MM-GBSA energy calculation

The stability of the Disogluside-tPA complex was also determined by calculating the binding free energy using the MM-GBSA approach. The estimated ΔG_bind value of -65.04 ± 4.82 kcal/mol suggests a good binding stability of Disogluside to the active site of the protein (Table 3). Breakdown of the total binding energy showed that van der Waals forces (ΔG_Vander = -44.75 ± 3.09 kcal/mol) predominated the binding, followed by considerable lipophilic forces (ΔG_Lipophilic = -25.92 ± 2.31 kcal/mol), which indicated the presence of a strong hydrophobic contribution to the binding affinity of Disogluside. Coulombic interactions (ΔG_Coulomb = -15.05 ± 2.88 kcal/mol) also played a role in electrostatic stabilization of the complex.

Table 3 — MM-GBSA energy calculation of Disogluside-tPA complex

S. No	Parameters	Binding Free Energy
1	ΔGbind	-65.04±4.82
2	ΔGcoulomb	-15.05±2.88
3	ΔGcovalent	-3.93±1.19
4	ΔGvander	-44.75±3.09
5	ΔGHbond	-1.98±0.25
6	ΔGLipophilic	-25.92±2.31

By contrast, hydrogen-bonding (ΔG_HBond = −1.98 ± 0.25 kcal/mol) and covalent contributions (ΔG_Covalent = −3.93 ± 1.19 kcal/mol) were comparatively small, although complementary, energy contributions. Taken together, these findings

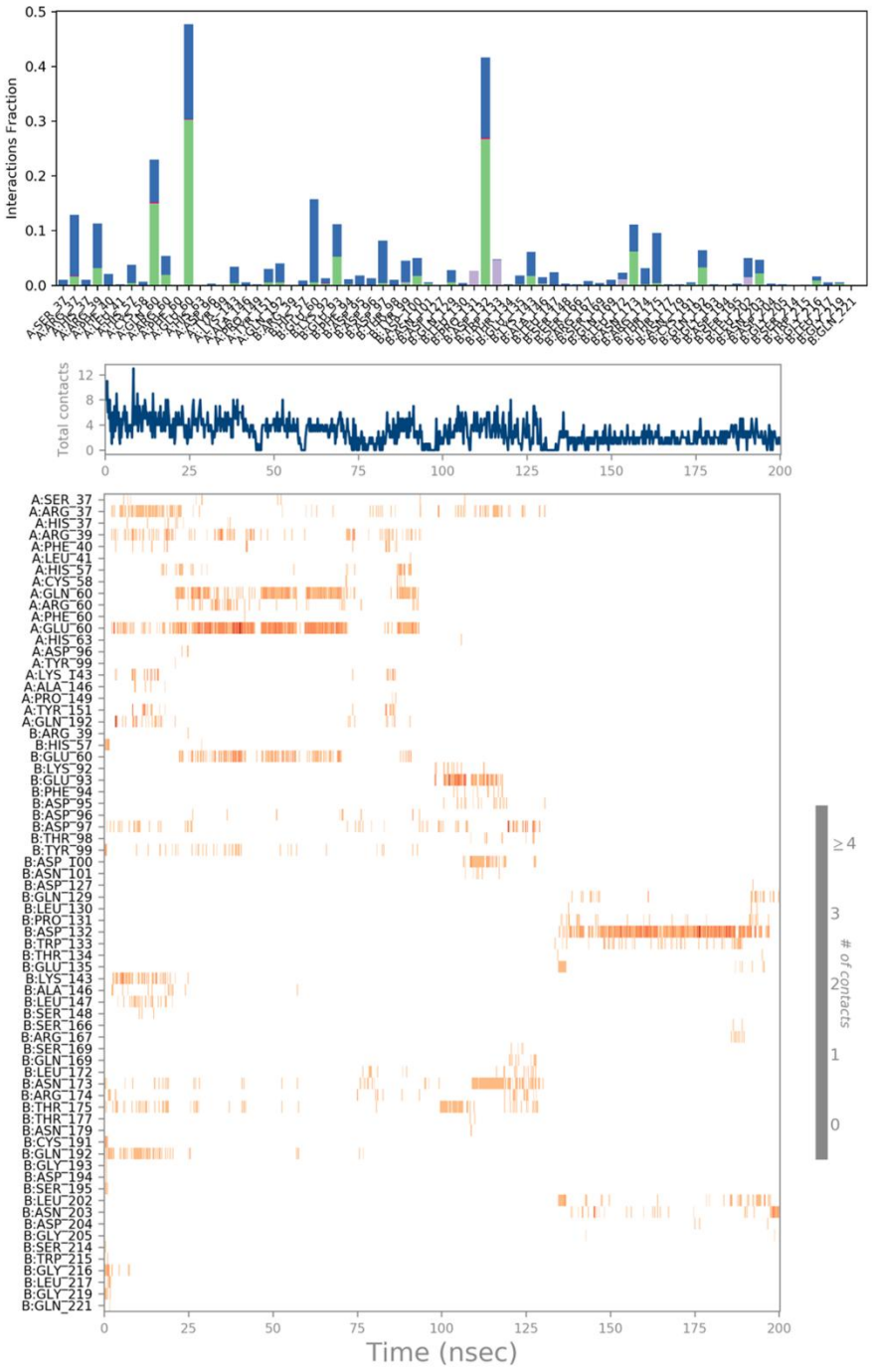

Fig. 9 — (a) Bar diagram; and (b) Timeline of disogluside with tissue tPA showing hydrogen bonding with key active site residues

suggest that the interaction of Disogluside with tPA is largely driven by hydrophobic and van der Waals forces; thus, Disogluside seems to be a robust candidate as an inhibitor.

Limitation and future prospective

The current *in silico* studies on phytoconstituents from *Paris polyphylla* as Tissue Plasminogen Activator inhibitors offer initial insights into binding affinity and potential binding modes; however, there are some limitations. Docking simulations use static protein structures and fail to account for protein flexibility, solvent effects, and other factors of the physiological milieu that affect ligand-protein binding. The binding affinities reported are calculated from scoring

functions, which may not correlate well with binding free energies and inhibitory activities.

Additionally, the research fails to consider *in vitro* pharmacokinetic and pharmacodynamic characteristics, essential for drug design. The polypharmacology of the phytoconstituents and off-target effects were also not considered. More importantly, the role of tPA in inflammation is multifaceted and may result in a therapeutic anti-inflammatory effect even if tPA is inhibited. Thus, the results of this *in silico* study need to be verified with rigorous *in vitro* enzymatic and *in vivo* tests to determine the efficacy and safety of the compounds with anti-inflammatory effects.

Conclusion

This study demonstrates that phytoconstituents of *Paris polyphylla*, particularly Disogluside, exhibit strong binding affinity and stable interaction with the active site of tPA. The combined docking, molecular dynamics simulation, and MM-GBSA analyses confirm that the Disogluside–tPA complex is structurally stable and energetically favorable, with binding predominantly driven by hydrophobic and van der Waals interactions. These findings support the potential of Disogluside as a promising lead compound for tPA inhibition and anti-inflammatory drug development. However, further *in vitro* and *in vivo* studies are necessary to validate its pharmacological efficacy and therapeutic applicability.

Acknowledgement

We thank all open-access computational servers that make this research possible. This work was supported by the Deanship of Scientific Research, Vice Presidency for Graduate Studies and Scientific Research, King Faisal University, Saudi Arabia [Grant No. KFU264382].

Conflict of interest

All authors declared no conflict of interest.

References

1 Chen L, Deng H, Cui H, Fang J, Zuo Z, Deng J, Li Y, Wang X & Zhao L, Inflammatory responses and inflammation-associated diseases in organs. *Oncotarget*, 9 (2018) 7204.

2 Yatsenko T, Skrypnyk M, Troyanovska O, Tobita M, Osada T, Takahashi S, Hattori K & Heissig B, The role of the plasminogen/plasmin system in inflammation of the oral cavity. *Cells*, 12 (2023) 1.

3 Seillier C, Hélie P, Petit G, Vivien D, Clemente D, Le Mauff B, Docagne F & Toutirais O, Roles of the tissue-type plasminogen activator in immune response. *Cell Immunol*, 371 (2022) 104451.

4 Lin L, Bu G, Mars WM, Reeves WB, Tanaka S & Hu K, TPA activates LDL receptor-related protein 1-mediated mitogenic signaling involving the P90RSK and GSK3β pathway. *Am J Pathol*, 177 (2010) 1687.

5 White S, Lin L & Hu K, NF-κB and TPA signaling in kidney and other diseases. *Cells*, 9 (2020) 1.

6 Klavina PA, Leon G, Curtis AM & Preston RJS, Dysregulated haemostasis in thrombo-inflammatory disease. *Clin Sci*, 136 (2022) 1809.

7 Didehvar K, Haghshenas M, Yarmohammadi R, Hajikarimloo B & Ghafoury R, Tissue plasminogen activator as an approved strategy for ischemic stroke: A review of TPA's structure, mechanism of action and the novel targeting methods. *J Mol Neurosci*, 75 (2025) 1.

8 Devi WJ, Laishram JM & Chakraborty S, Antioxidant activity and polyphenol contents of Paris polyphylla Smith and prospects of in situ conservation. *Int J Curr Microbiol Appl Sci*, 7 (2018) 2355.

9 Kshetrimayum V, Heisnam R, Keithellakpam OS, Radhakrishnanand P, Akula SJ, Mukherjee PK & Sharma N, Paris polyphylla Sm. induces reactive oxygen species and caspase 3-mediated apoptosis in colorectal cancer cells *in vitro* and potentiates the therapeutic significance of fluorouracil and cisplatin. *Plants*, 12 (2023) 1.

10 Rawat JM, Pandey S, Rawat B, Rai N, Preeti P, Thakur A, Butola JS & Bachheti RK, Traditional uses, active ingredients, and biological activities of Paris polyphylla Smith: A comprehensive review of an important Himalayan medicinal plant. *J Chem*, 2023 (2023) 7947224.

11 Singh PP, Structure-based virtual screening of phytochemicals from Phyllanthus amarus as potent inhibitory phytocompounds against Marburg virus disease. *Eur J Med Adv*, 3 (2023) 23.

12 Vemula D, Maddi DR & Bhandari V, Homology modeling, virtual screening, molecular docking, and dynamics studies for discovering Staphylococcus epidermidis FtsZ inhibitors. *Front Mol Biosci*, 10 (2023) 1.

13 Halgren TA, Merck molecular force field. I. Basis, form, scope, parameterization, and performance of MMFF94. *J Comput Chem*, 17 (1996) 490.

14 Rainsford KD & Consensus Report Group on Nimesulide, Nimesulide–a multifactorial approach to inflammation and pain: Scientific and clinical consensus. *Curr Med Res Opin*, 22 (2006) 1161.

15 Renatus M, Bode W, Huber R, Stürzebecher J, Prasa D, Fischer S, Kohnert U & Stubbs MT, Structural mapping of the active site specificity determinants of human tissue-type plasminogen activator: Implications for the design of low molecular weight substrates and inhibitors. *J Biol Chem*, 272 (1997) 21713.

16 Laskowski RA, Jabłońska J, Pravda L, Vařeková RS & Thornton JM, PDBsum: Structural summaries of PDB entries. *Protein Sci*, 27 (2018) 129.

17 Kurmi SPC, Thapa S, Mahmood AAR, Murav AK, Biradar MS, Bhagyanath N & Maurya SN, Medicinal chemistry insights of molecular docking and cell permeability mechanism of phytoconstituents present in Mimosa pudica as NS2B-NS3 protease inhibitors against dengue virus. *Discover Chem*, 2 (2025) 78.

18 Trott O & Olson AJ, AutoDock Vina: Improving the speed and accuracy of docking with a new scoring function, efficient optimization, and multithreading. *J Comput Chem*, 31 (2009) 455.

19 O'Boyle NM, Banck M, James CA, Morley C, Vandermeersch T & Hutchison GR, Open Babel: An open chemical toolbox. *J Cheminform*, 3 (2011) 1.

20 Kurmi SPC, Thapa S, Metri SM, Biradar MS, Esther VA, Murav AK & Maurya SN, Molecular docking, drug-likeness properties, and toxicity prediction of alkaloidal phytoconstituents of Piper longum against monoamine oxidase enzyme-A as an anti-depressive agent. *Discover Chem*, 2 (2025) 1.

21 Fährrolfes R, Bietz S, Flachsenberg F, Meyder A, Nittinger E, Otto T, Volkamer A & Rarey M, Proteins Plus: A web portal for structure analysis of macromolecules. *Nucleic Acids Res*, 45 (2017) W337.

22 Hasan MM, Khan Z, Chowdhury MS, Khan MA, Moni MA & Rahman MH, *In silico* molecular docking and ADME/T analysis of quercetin compound with its evaluation of broad-spectrum therapeutic potential against particular diseases. *Inform Med Unlocked*, 29 (2022) 100894.

23 Lipinski CA, Lombardo F, Dominy BW & Feeney PJ, Experimental and computational approaches to estimate solubility and permeability in drug discovery and development settings. *Adv Drug Deliv Rev*, 23 (1997) 3.

24 Daina A, Michielin O & Zoete V, SwissADME: A free web tool to evaluate pharmacokinetics, drug-likeness and medicinal chemistry friendliness of small molecules. *Sci Rep*, 7 (2017) 42717.

25 Swaroop K, Renukaradhya M, Shaik S, Thatipelli RC, Krishna KVS, Sangi SMA, Islam MM, Meravanige G, Sreeharsha N, Chohan MS, Thapa S, Akin-Adewumi A & Atoki AV, Evaluation of the anti-inflammatory potential of atorvastatin targeting TNF-α, IL-6, and IL-1β using integrated *in vitro* and *in silico* approaches. *Sci Rep*, 16 (2026) 9914.

26 Yogesh HS, Shaik S, Sangi SMA, Swaroop K, Nagaraja S, Anitha KN, Mishra VK, Kurmi SPC, Nath S & Thapa S, Polyphenol-based therapeutics for glioblastoma: Validation from in-vitro cell viability assay and integrated onco-omics computational analysis. *Naunyn Schmiedebergs Arch Pharmacol*, 399 (2026) 3969.

27 Nyambo K, Tapfuma KI, Adu-Amankwaah F, Julius L, Baatjies L, Niang IS, Smith L, Govender KK, Ngxande M, Watson DJ, Wiesner L & Mavumengwana V, Molecular docking, molecular dynamics simulations and binding free energy studies of interactions between Mycobacterium tuberculosis Pks13, PknG and bioactive constituents of extremophilic bacteria. *Sci Rep*, 14 (2024) 1.

28 Hollingsworth SA & Karplus PA, A fresh look at the Ramachandran plot and the occurrence of standard structures in proteins. *Biomol Concepts*, 1 (2010) 271.